THE NUMERICAL ANALYSES OF THE FLOW STRUCTURE IN AN ANNULAR SPACE PARTIALLY-OBSTRUCTED

Bruno Venturini Loureiro
Laboratório de Fenômenos de Transporte, UCL – Faculdade do Centro Leste, Serra - ES
brunovl@ucl.br

Reginaldo Rosa Cotto de Paula
Centro Federal de Educação Tecnológica do Espírito Santo – CEFET-ES, Vitória - ES
reginaldo@cefetes.br

Abstract *In this work the effects of the height of the bed and internal cylinder rotation on flow structure in a concentric annular region have been studied using the standard k - ε turbulence model. The aim of this study is to develop a benchmark for research in drilling process of oil and gas wells. In order to investigate the influence of the height of the bed and inner cylinder rotation on flow structure, the following idealized cases have been considered: (i) 2-D steady flow with water as work fluid, (ii) four different heights of the bed, (iii) four different inner cylinder angular rotation velocities, and (iv) a plate parallel to the axis of rotation as the bottom of the annular space. In this case, the circumferential symmetry of the annular space was lost. The results of the numerical analysis showed that the height of the bed has smaller influence on the velocity field, wall shear stress and flow structure in the annular region than the angular velocity of the inner cylinder..*

Keywords*: turbulence model, obstructed annular flow, wall shear stress*

1. INTRODUCTION

Considerable research has been directed toward quantifying the influence of inner cylinder rotation in concentric annular geometries. This research is typical of many industrial and engineering applications, such as drilling operations in the oil and gas industry. Although the influence of the height of the bed on the turbulent flow structure in a concentric rotating system is very important, few works have been reported in the literature.

On the last decades, numerous experimental and numerical studies of concentric annular flow have been carried out (Rehme, 1974; Satake and Kawamura, 1993; Kannepalli and Piomelli, 2000). The problem of the stability of viscous flow between two concentric rotating cylinders was first investigated mathematically and experimentally by Taylor in 1923. It was observed that when internal cylinder was stationary and external cylinder was rotated, the flow was stable, however, when the inner cylinder was rotated and the outer cylinder was stationary, the flow behavior was unstable. In addition, Taylor observed that the increase of the fluid viscosity can delay the instability. Kaye and Elgar (1958) performed experiments to study the combined axial and rotational flow in an annular with the rotating inner wall. They identified four different flow regimes in the annular gap: laminar flow; laminar flow with vortices, turbulent flow; and turbulent flow with vortices. Nouri et al. (1993) and Escudier et al. (1995) performed an experimental investigation in concentric annular channel to observe the flow pattern of Newtonian and non-Newtonian fluids. Azouz and Shirazi (1998) examined the performance of several turbulent models to calculate the turbulent flow in concentric annuli, and compared their results with the experimental data of Nouri et al. (1993). Chung et al. (2002) carried out direct numerical simulation (DNS) for a turbulent concentric annular pipe flow at low Reynolds number. They found that turbulent structures near the outer wall were more activated than those near the inner wall, which may be attributed to the different vortex regeneration process between the inner and outer walls. Loureiro et al. (2006) and Loureiro and Siqueira (2006) carried out experiments in order to investigate the effect of the inner cylinder rotation in the annular space partially obstructed. In addition, the authors to analyze the influence of height of the particles bed on the process of drilling of gas and oil. The results showed that the rotation of the inner cylinder causes the movement and compactation of the bed.

In this study, a turbulent 2-D rotating flow in a concentric annuls was simulated using k- ε turbulence model in order to investigate the effect of rotation of the inner cylinder on the flow structure. The objective of the present study is to analyze the influence of the height of the bed and angular velocity on velocity field and wall shear stress due to the rotation of the inner cylinder. In this case, the bottom of the annular space was considered a plate parallel to the axis of rotation. Thus, the circumferential symmetry of the annular space was lost.

2. BASIC EQUATIONS AND NUMERICAL PROCEDURE

In the present work, to express the physical phenomena that occurs in a turbulent rotating flow in an annular space partially-obstructed, four different heights of the beds were studied: H/R_o = 0.47; (b) H/R_o = 0.74; (c) H/R_o = 1.00; and (d) H/R_o = 1.26, where H is the bed level and Ro is the outer radius, as shown in Fig. 1. In addition, four different angular velocities of rotation of the inner cylinder were simulated: Ω_i = 10 rad/s; Ω_i = 14 rad/s; Ω_i = 18 rad/s and Ω_i = 22 rad/s. A schematic diagram of the two dimensional physical models and coordinate system is shown in Fig. 1. The inner radius was R_i = 0.0825 m and the outer radius was R_o = 0.157 m. The bottom of the annular space was a plate parallel to the axis of rotation, where, $x < 0$ represents the upstream bed, and $x > 0$ represents the downstream bed of the obstruction. The idealized bed profiles were based on the previous experimental studies carried out by Loureiro et al. (2006) and Loureiro and Siqueira (2006). The experiments were conducted in an annular flow erosion simulator. Its working section was a 2.0 m long annular tube.

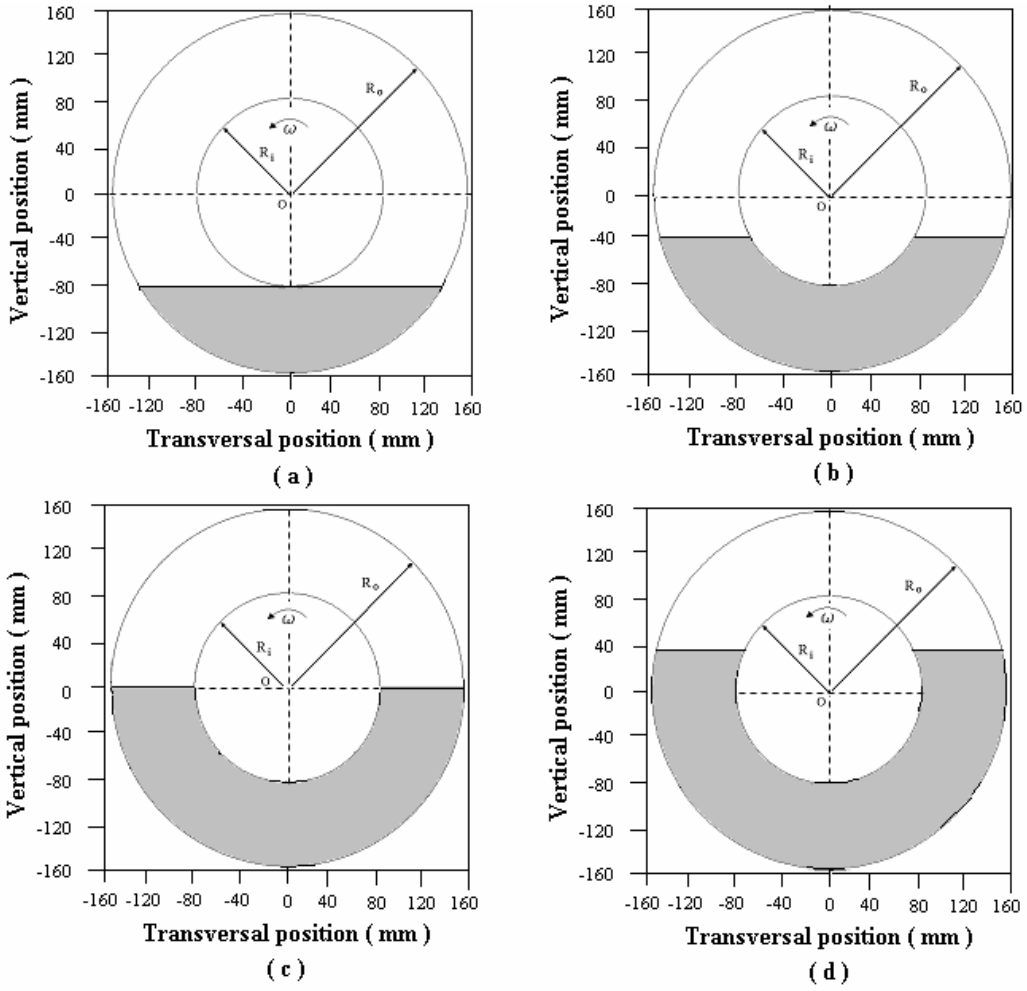

Figure 1. Schematics representation of the physical models: (a) H/R_o = 0.47; (b) H/R_o = 0.74; (c) H/R_o = 1.00; and (d) H/R_o = 1.26.

In this analysis a steady flow was assumed and the standard k-epsilon model was used to solve the transport equations of turbulent kinetic energy and its dissipation ratio defined as:

$$\frac{\partial}{\partial x_i}(\rho k u_i) = \frac{\partial}{\partial x_i}\left[\left(\mu + \frac{\mu_t}{\sigma_k}\right)\frac{\partial k}{\partial x_j}\right] + G_k - \rho\varepsilon \tag{1}$$

$$\frac{\partial}{\partial x_i}(\rho\varepsilon u_i) = \frac{\partial}{\partial x_j}\left[\left(\mu + \frac{\mu_\varepsilon}{\sigma_\varepsilon}\right)\frac{\partial \varepsilon}{\partial x_j}\right] + C_{1\varepsilon}\frac{\varepsilon}{k}G_k - C_{2\varepsilon}\rho\frac{\varepsilon^2}{k} \tag{2}$$

In these Eqs. (1) and (2), ρ is the fluid density, μ is the laminar viscosity, μ_t is the turbulent viscosity, σ_k, σ_ε are the turbulent Prandtl number for *k* and ε, respectively and G_k represents the generation of turbulent kinetic energy due to the mean velocity gradients. The turbulent viscosity, μ_t is computed by combining *k* and ε as follows:

$$\mu_t = \rho C_\mu \frac{k^2}{\varepsilon} \tag{3}$$

where C_μ is a constant. The model constants $C_{1\varepsilon}$, $C_{2\varepsilon}$, σ_k, σ_ε and C_μ have the following default values: $C_{1\varepsilon}$ = 1.44; $C_{2\varepsilon}$ = 1.92; σ_k = 1.0; σ_ε = 1.3 and C_μ = 0.09.

In this work the Fluent 6.12.16 commercial program was used for numerical simulation. The flow equations in the program were discretized using a Control Volume Method (Fluent 6.1 User´s Guide, 2006). The SIMPLE algorithm of Patankar (1980) was used to obtain velocity and pressure fields and Power-Law discretization scheme for continuity, turbulent kinetic energy and its dissipation ratio. The boundary conditions for this problem were: no-slip conditions for all wall boundary contours: downstream and upstream beds, inner and outer cylinders. In the simulations it was used water as fluid of work. The Reynolds number of 1.1 x 10^3 was based on the following definition:

$$\mathrm{Re} = \frac{U_b(R_o - R_i)}{\nu} \tag{4}$$

where U_b is the bulk velocity and ν is the fluid viscosity.

3. RESULTS

In the present work, the influence of the height of the bed and inner cylinder rotation on the turbulence quantities in an annular space partially-obstructed was estimated for four heights of bed and four angular velocities using the standard k-ε turbulence model.

3.1. Determination of the Mesh dimension

In order to define the mesh dimension to be used in the numerical simulation, it is necessary to establish the grid independency. A comparison of nine numerical simulations was made using three different meshes for each height of bed, called coarse, regular and fine meshes. In this case, the influence of grid refinement, in all numerical simulations, was evaluated using both the estimated tangential velocity and wall shear stress. In addition, computations of turbulent flow were performed only for Ω_i = 18 rad/s. Table 1 shows the specifications of the mesh for each height of bed used in this study.

Table 1. Specification of mesh dividing for the computational domain.

		***H/R*$_o$ = 0.47**	
Mesh	**Nodes**	**CONVERGENCE**	**CPU TIME**
Coarse	21118	11800 iterations	3h 16 min
Regular	30261	14500 iterations	4h 01 min
Fine	43839	23900 iterations	6h 38 min
		***H/R*$_o$ = 0.74**	
Coarse	72721	15401 iterations	4h 16 min
Regular	163081	29000 iterations	11h
Fine	234577	48500 iterations	26 h 56 min
		***H/R*$_o$ = 1.00**	
Coarse	72721	18501 iterations	5h 08 min
Regular	163081	43600 iterations	12h 06 min
Fine	234577	63800 iterations	35 h 26 min
		***H/R*$_o$ = 1.26**	
Coarse	46657	18101 iterations	5h
Regular	66932	26201 iterations	7h 16 min
Fine	96188	37301 iterations	20 h 43 min

Figure 2 shows the results of the estimated tangential velocity profiles along radial coordinate, at $x = 0$, obtained using the standard k-ε model for the coarse, regular and fine meshes for the four different bed heights studied. The results of the grid refinement for the 2-D simulations showed the same values of the velocity profiles for the coarse, regular and fine meshes. All the results of the numerical simulations suggested an independence of the mesh size on the velocity profiles. Therefore, in the sections (3.2) and (3.3), only the simulations with the regular mesh will be presented due to low computational cost and CPU time required.

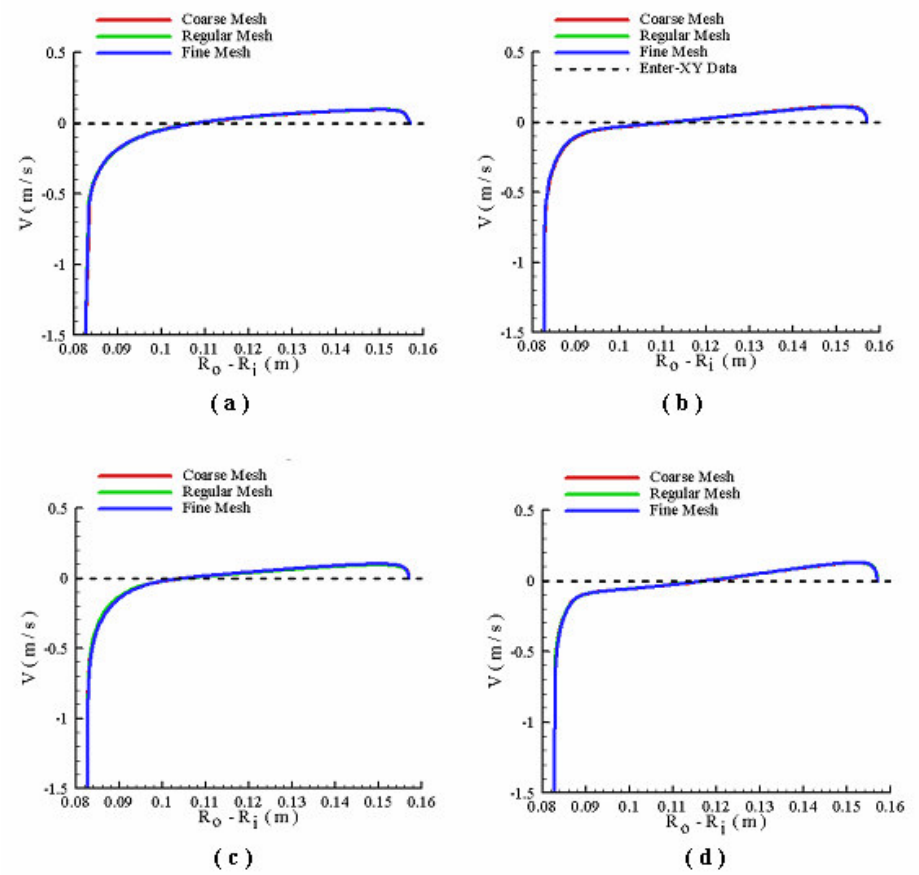

Figure 2. Results of the meshes test of mean velocity profiles in the radial direction, $R_o - R_i$, plotted at $x = 0$: H/R_o = 0.47; (b) H/R_o = 0.74; (c) H/R_o = 1.00; and (d) H/R_o = 1.26.

Figure 3 shows the results of the estimated wall shear stress in the upstream bed of the obstruction ($\sim x < 0$) for the tree different meshes tested. In the Fig. 3 (a), at H/R_o = 0.47, the results of the grid refinement for the numerical simulations showed a small difference in the wall shear stress profiles obtained using fine, regular and coarse meshes. In the Figs. 3 (b) and (d), at H/R_o = 0.74 and H/R_o = 1.26, respectively, the results obtained using the fine mesh were similar to those obtained using the regular mesh. In the Fig. 3 (c), at H/R_o = 1.00, the grid refinement for the numerical simulations presented the same values of the wall shear stress for between results obtained using fine and regular meshes.

These results of the 2-D numerical simulations suggested that the independence of the grid refinement on the values of the wall shear stress were obtained with the regular and fine meshes, although there were small differences among the values obtained with the coarse mesh in all simulations.

3.2. Effect of height bed on turbulence structure

In this section, the effect of increase on bed level on turbulence structure was analyzed. Figure 4 presents the streamlines of the velocity at H/R_o = 0.47; (b) H/R_o = 0.74; (c) H/R_o = 1.00; and (d) H/R_o = 1.26, respectively. According to Fig. 4, a different behavior of the recirculation in the annular space, $R_o - R_i$, is observed due to the influence of the variation of the height of the bed. In addition, a significant concentration of the streamlines is seen in the upstream region of obstruction near the bed level. This fact has serious implications on the prediction of the shear

stress in the annular space. Since the streamlines concentration causes the difference between the shear stress in the upstream and downstream beds of the obstruction.

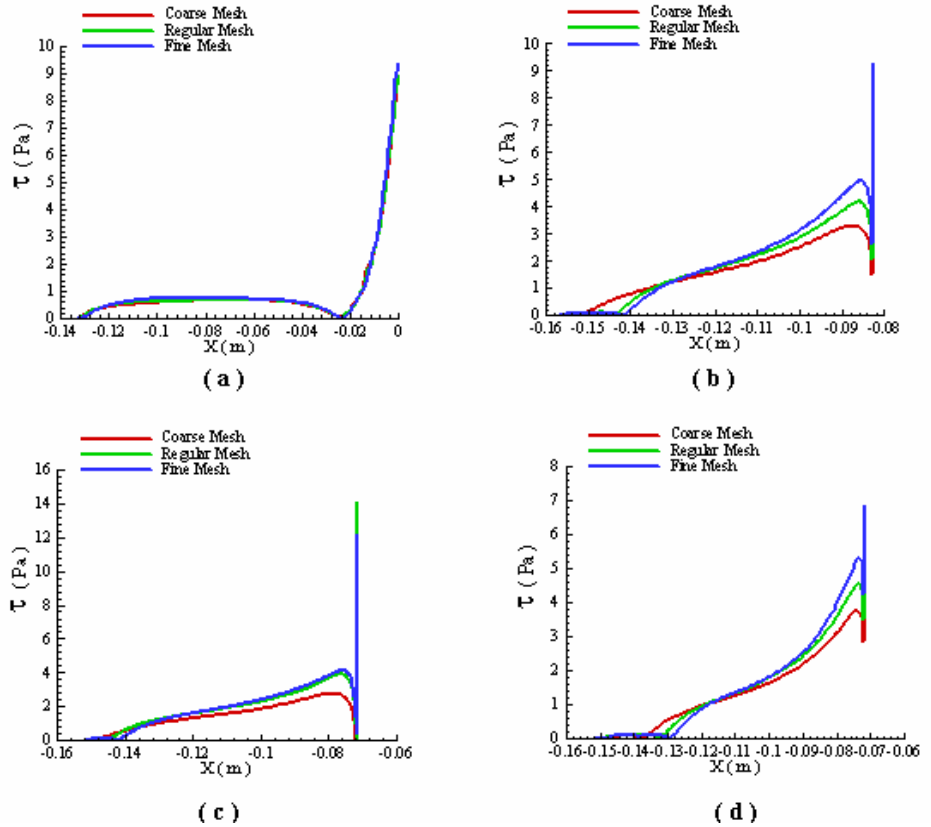

Figure 3. Results of the meshes test of wall shear stress profiles in the upstream region of the obstruction: (a) H/R_o = 0.47; (b) H/R_o = 0.74; (c) H/R_o = 1.00; and (d) H/R_o = 1.26.

Figure 5 shows the comparisons among the estimated tangential velocity profiles for the four different bed heights investigated. From these results it was found that the increase of the bed height do not influence the tangential velocity profiles, at $x = 0$, for the angular velocity established.

Figure 6 shows the comparisons among the estimated wall shear stress profiles in the upstream bed of the obstruction ($\sim x < 0$) for the four different heights of the bed investigated. Figure 6 shows that the peak values of the wall shear stress occurred near the inner wall. This effect occurred due to inner cylinder rotation.

Figure 7 shows the comparisons among the estimated wall shear stress profiles in the downstream bed of the obstruction ($\sim x > 0$) for the several bed heights investigated. From these results it was found that, due to inner cylinder rotation, the peak values of the wall shear stress occurred near the inner wall. It is interesting to note that the generated shear stress at H/R_o = 0.74; H/R_o = 1.00; and H/R_o = 1.26 presented the same magnitude order. However, for bed level H/R_o = 0.47, the shear stress was very small compared to those obtained by the other bed levels, except very close to the outer wall. The comparisons between the results of Figs. 6 and 7 show that the predicted shear stress in the downstream beds of the obstruction region were much smaller than the obtained in the upstream beds, independent of the height of the bed investigated. As shown in Figs. 6 and 7 the inner cylinder rotation effect induces the non-zero shear stress near the inner wall of the annular space partially obstructed.

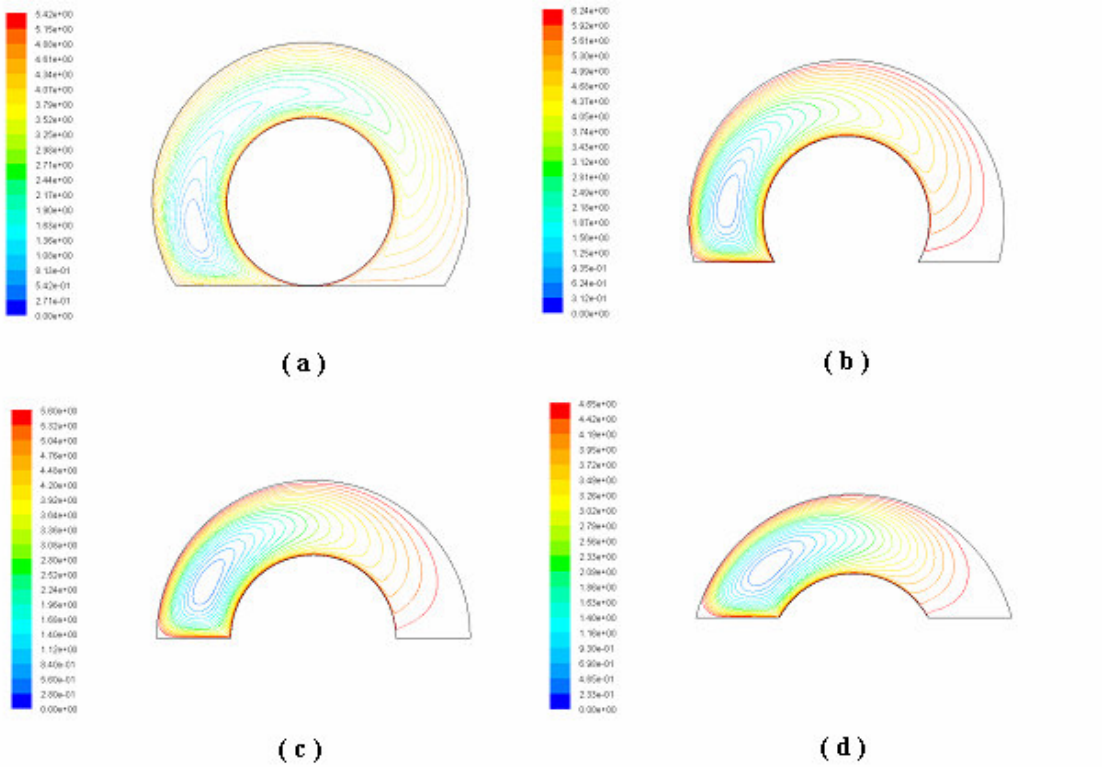

Figure 4. Streamlines of velocity for : (a) H/R_o = 0.47; (b) H/R_o = 0.74; (c) H/R_o = 1.00; and (d) H/R_o = 1.26.

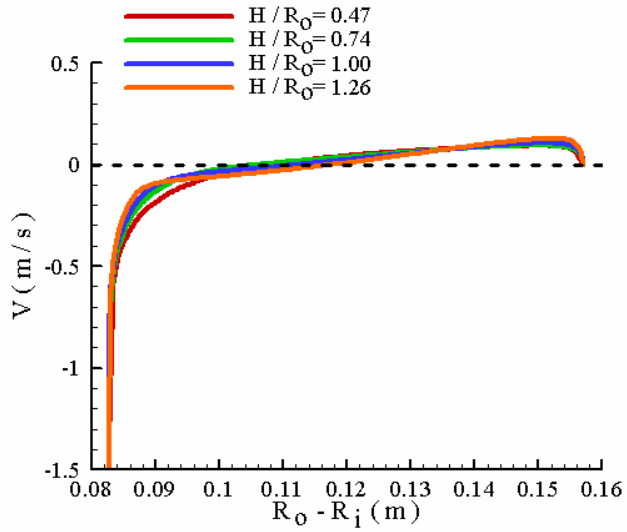

Figure 5. Estimated tangential velocity profiles in the radial direction, $R_o - R_i$, plotted at x = 0 for different bed heights for Ω_i = 18 rad/s.

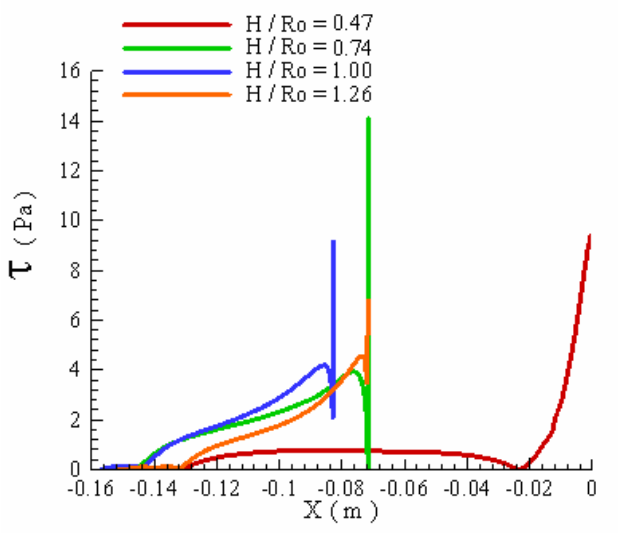

Figure 6. Estimated wall shear stress profiles on the upstream bed to the four different heights of the beds investigated (Ωi = 18 rad/s).

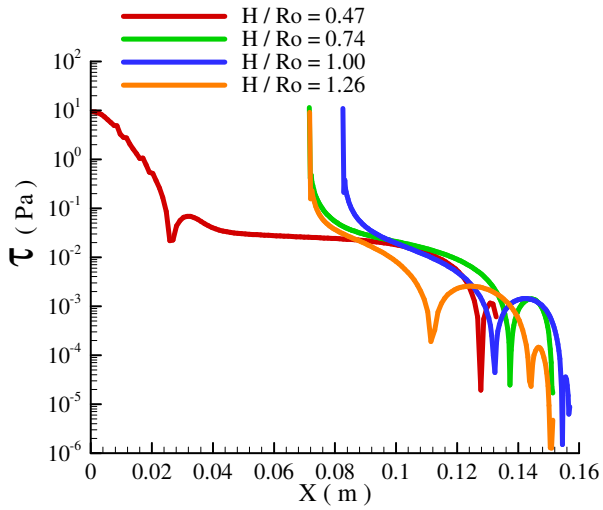

Figure 7. Estimated wall shear stress profiles on the downstream bed for the four different heights of the bed investigated (Ωi = 18 rad/s).

3.3. Effect of rotation of the inner cylinder on turbulence structure

In this section, the effects of the angular velocity for each height of the bed investigated were analyzed. Figure 8 shows the results of the estimated tangential velocity profiles for the four bed levels: (a) (a) H/R_o = 0.47; (b) H/R_o = 0.74; (c) H/R_o = 1.00; and (d) H/R_o = 1.26 and for the four angular velocities: Ω_i = 10 rad/s; Ω_i = 14 rad/s; Ω_i = 18 rad/s and Ω_i = 22 rad/s studied. In all cases the tangential velocity changed very little with the increase in the angular velocity, except in the region near of the inner cylinder, as shown Fig. 8.

Figure 9 shows the results of the estimated shear stress on the upstream bed of the obstruction (~ x < 0) for several angular velocities. It is seen from Fig. 9 that in all cases, the increase of the inner cylinder rotation amplified the effect of the shear stress over upstream bed and the stress magnitude over all the heights of the bed investigated. The rotation effect induces large values of the shear stress near the inner cylinder.

Figure 10 shows the results of the estimated shear stress on the downstream bed of the obstruction (~ x > 0). The results suggested that there is not significant change in the shear stress with increase of the inner cylinder rotation for the bed levels of H/R_o = 0.74; H/R_o = 1.00; H/R_o = 1.26. However, it occurred a great variation of the shear stress in the region near the inner cylinder, as shown in Fig. 9 10 (b), (c) and (d), respectively. It was interesting to note, in the Fig. 10 (a), that the same behavior was not observed in the bed level H/Ro = 0.47.

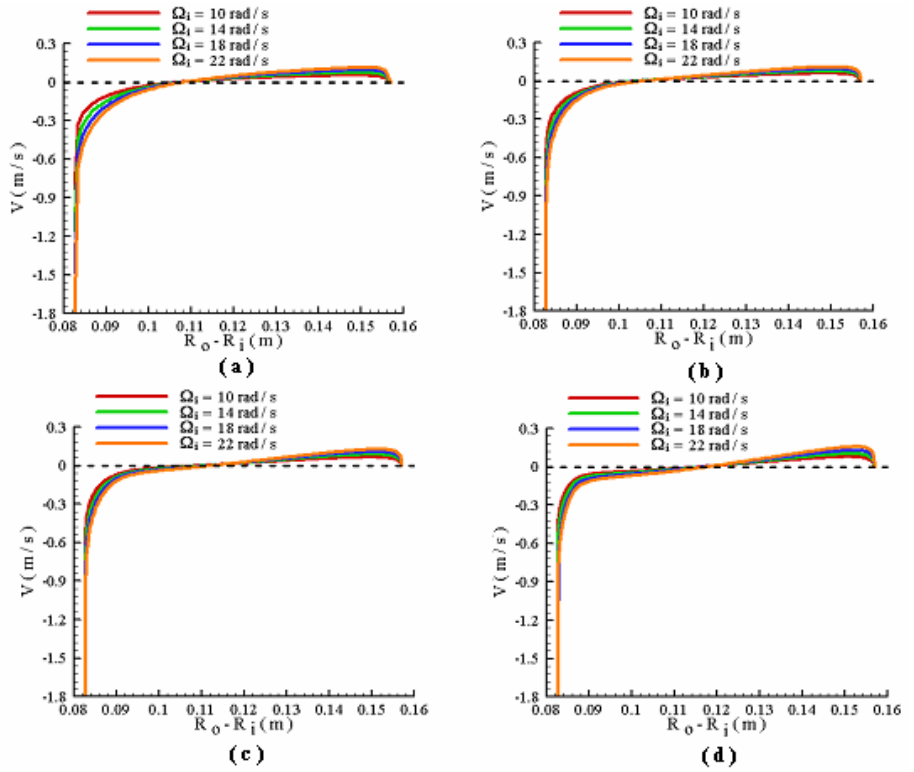

Figure 8. Estimated tangential velocity profiles in the radial direction, $R_o - R_i$, plotted at $x = 0$ for four different angular velocities: (a) $H/R_o = 0.47$; (b) $H/R_o = 0.74$; (c) $H/R_o = 1.00$; and (d) $H/R_o = 1.26$.

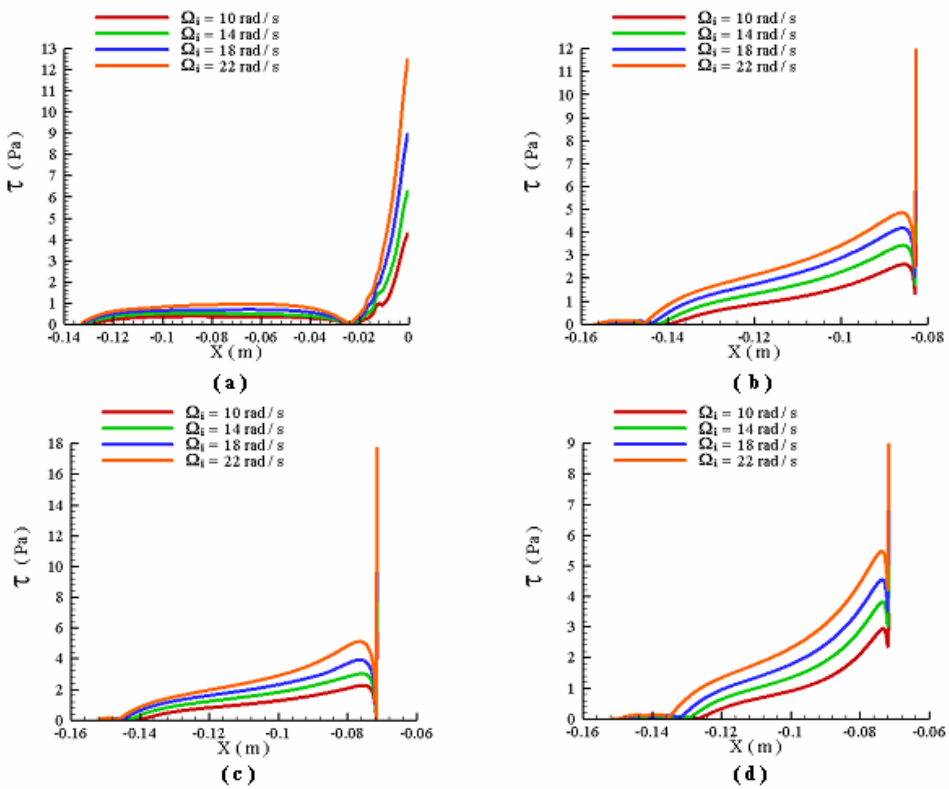

Figure 9. Estimated wall shear stress profiles on the upstream bed for the four different angular velocities investigated: (a) $H/R_o = 0.47$; (b) $H/R_o = 0.74$; (c) $H/R_o = 1.00$; and (d) $H/R_o = 1.26$.

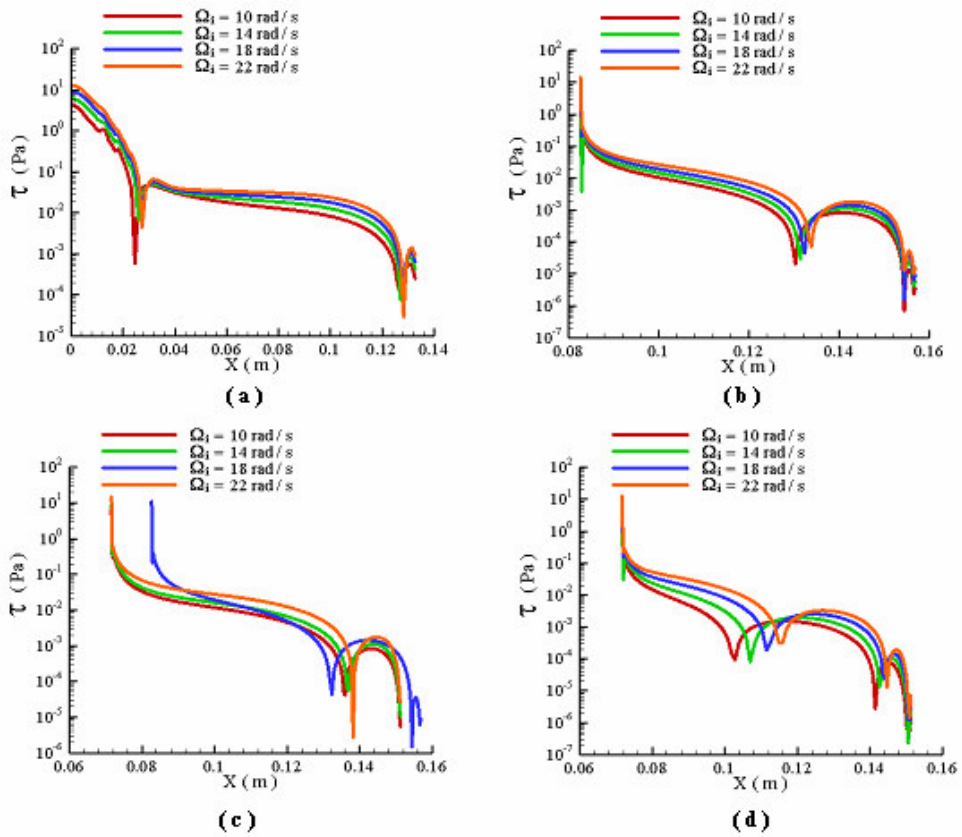

Figure 10. Estimated wall shear stress profiles on the downstream bed for the four different angular velocities investigated: (a) H/R_o = 0.47; (b) H/R_o = 0.74; (c) H/R_o = 1.00; and (d) H/R_o = 1.26.

4. CONCLUSIONS

The 2-D turbulent flow in a rotating concentric annular space partially obstructed was investigated numerically by using the standard k - ε turbulence model. Several cases of numerical simulations were conducted in order to examine the influence of mesh resolution and the effect of the bed level in the velocity and shear stress profiles due to inner cylinder rotations. The main results of this study were summarized as follows:

(I) The mesh refinement for the velocity field showed a grid independence on mesh size. Although, there are differences between the distribution of the shear stress obtained by the coarse mesh and those obtained using the regular and fine meshes, the grid refinement did not show any significant difference on the results of shear stress obtained with the regular and fine meshes.

(II) Numerical investigation revealed a significantly concentration of the streamlines in the upstream region of the obstruction near the bed. This concentration of the streamlines causes the difference between the shear stress in the downstream and upstream regions.

(III) The numerical simulation showed that the four different heights of the beds investigated did not influenced the tangential velocity profiles for the inner cylinder rotation of Ω_i = 18 rad/s. The shear stress at H/R_o = 0.74; H/R_o = 1.00; and H/R_o = 1.26 presented the same magnitude order in the downstream region. However, for the bed level, H/R_o = 0.47, the shear stress was very small when compared to those obtained by the other bed levels, except very close to the outer wall.

(IV) The results of the numerical simulation suggested that the large values of shear stress near the inner walls of the upstream and downstream beds of the obstruction region should be attributed to rotation of the inner cylinder.

(V) The increase of the angular velocity did not have significant influence on the tangential velocity, except in the region near to inner cylinder.

(VI) The increase of the inner cylinder rotation amplified the effect of the shear stress on upstream bed and the stress magnitude over all the heights of the bed investigated.

(VII) It was found that there was not significant change in the shear stress on the downstream bed with increase of the inner cylinder rotation for the bed levels of H/R_o = 0.74; H/R_o = 1.00; H/R_o = 1.26. However, it occurred a great variation of the shear stress in the region near the inner cylinder. This same behavior was not observed in the bed level of H/Ro = 0.47.

(VIII) The results of this work can be used in order to help the development and improvement of turbulent flow models in a concentric annular region and on application of this flow to the drilling process of oil and gas wells.

5. ACKNOWLEDGEMENTS

The authors acknowledge to FAPES – Fundação de Apoio à Ciência e Tecnologia do Espírito Santo (Grant 30899702/2005).

6. REFERENCES

Azouz, I. and Shirazi, S.A., 1998, "Evaluation of several turbulence models for turbulent flow in concentric and eccentric annuli", ASME: Jurnal of Energy Resour., Technol, Vol. 120, pp. 268-275.

Chung, S.Y., Rhee, G.H. and Sung, H.J., 2002, "Direct numerical simulation of turbulent concentric annular pipe flow. Part I: Flow field", International Journal of Heat Fluid Flow, Vol. 23, pp. 426-440.

Escudier, M.P., Gouldson, I.W. and Jones, D.M., 1995, "Flow of shear-thinning fluids in a concentric annulus", Exp. Fluids, 18, pp. 225-238.

Kannepalli. C. and Piomelli, U., 2000, "Large-eddy simulation of a three-dimensional shear-driven turbulent boundary layer", Journal of Fluid Mechanic, Vol. 423, pp. 175-203.

Kaye, J. and Elgar, E.C., 1958, "Modes of adiabatic and diabatic fluid flow in an annulus with an inner rotating cylinder". Transf. ASME: Journal of Heat Transfer, Vol. 80, pp. 753-765.

Loureiro, B.V., Siqueira, R.N. and Fontenelle, F.C.N., 2006, "Efeito da Rotação da Coluna de Perfuração na Supensão de Cascalhos Sedimentados em Poços Horizontais", Encontro Nacional de Hidráulica de Perfuração e Completação de Poços de Petróleo e Gás, Domingos Martins, Brazil.

Loureiro, B.V. and Siqueira, R.N., 2006, "Sediment particle entrainment in na obstructed annular", Proceedings of the 11th Brazilian Congress of Thermal Sciences and Engineering, Curitiba, Barzil, p. 199.

Nouri, J.M., Umur, H. and Whitelaw, J.H., 1993, "Flow of Newtonian and non-Newtonian fluids in concentric and eccentric annuli", Journal of Fluid Mechanic, Vol. 253, pp. 617-641.

Rehme, K., 1974, "Turbulent flow in smooth concentric annuli with small radius ratios", Journal of Fluid Mechanic, Vol. 64, pp. 263-287.

Satake, S. and Kawamura, H., 1993, "Large eddy simulation of turbulent flow in concentric annuli with a thin inner rod", In: Proceedings of the 9th Symposium on Turbulent Shear Flows, pp. 5.5.1 – 5.5.6.

7. RESPONSIBILITY NOTICE

The authors are the only responsible for the printed material included in this paper.